Applied Radiation and Isotopes 135 (2018) 19–27

Contents lists available at ScienceDirect

Applied Radiation and Isotopes

journal homepage: www.elsevier.com/locate/apradiso

Automated radiosynthesis of Al[^{18}F]PSMA-11 for large scale routine use

Ken Kersemans[a,*], Kathia De Man[a], Jan Courtyn[a], Tessa Van Royen[b], Sarah Piron[b], Lieselotte Moerman[a], Boudewijn Brans[a], Filip De Vos[b]

[a] Ghent University Hospital, Nuclear Medicine, De Pintelaan 185, Ghent, Belgium
[b] Laboratory of Radiopharmacy, Ghent University, Ottergemsesteenweg 460, Ghent, Belgium

HIGHLIGHTS

- Critical parameters for the manual radiosynthesis of Al[^{18}F]PSMA-11 were optimized.
- Large scale automated radiosynthesis of Al[^{18}F]PSMA-11: up to 30 GBq/batch.
- Shelf life stability was determined in various conditions.
- Quality of the end product conforms to Ph. Eur. Guidelines.

ARTICLE INFO

Keywords:
PSMA
Prostate cancer
Automation
AlF^{2+}
Chelation

ABSTRACT

Objectives: We report a reproducible automated radiosynthesis for large scale batch production of clinical grade Al[^{18}F]PSMA-11.

Methods: A SynthraFCHOL module was optimized to synthesize Al[^{18}F]PSMA-11 by Al[^{18}F]-chelation. Results Al[^{18}F]PSMA-11 was synthesized within 35 min in a yield of 21 ± 3% (24.0 ± 6.0 GBq) and a radiochemical purity > 95%. Batches were stable for 4 h and conform the European Pharmacopeia guidelines.

Conclusions: The automated synthesis of Al[^{18}F]PSMA-11 allows for large scale production and distribution of Al[^{18}F]PSMA-11.

1. Introduction

Among men, prostate cancer (PCa) is the tumor with the second highest incidence rate in the world (15.0% of all reported cases) with an estimated 4 million men suffering from PCa according to the World Health Organisation (Stewart and Wild, 2014). An important problem in the clinical management is the development of tumor recurrence after prostatectomy or external beam radiation therapy with curative intent. One of the key issues herein is the early detection of recurrent disease (Aus et al., 2005).

In this context, innovative imaging methods have been developed aimed at the prostate specific membrane antigen (PSMA), a cell surface protein that is significantly overexpressed in PCa cells, as compared to other PSMA-expressing tissues (Hillier et al., 2009; Eder et al., 2012; Schäfer et al., 2012; Bander, 2006; Liu et al., 1997; Sweat et al., 1998; Mannweiler et al., 2009). Although PSMA is expressed in healthy prostate tissue too, it was shown that the expression strongly increases from benign epithelium to malignant neoplasia. Amongst the methods available to image PSMA-expressing tumors, the recently developed radiotracer Glu-NH-CO-NH-Lys-(Ahx)-[^{68}Ga(HBED-CC)] (^{68}Ga-PSMA-11) as a ^{68}Ga-labeled PSMA-targeted radioligand became well-established across many countries (Maurer et al., 2016).

Unfortunately, ^{68}Ga-labeled compounds are produced with in-house generators that provide limited activity per synthesis. Thus, depending on the lifespan of the generator, only 1–4 patient doses per elution can be produced. Each of these elutions requires a separate synthesis at different times of the day. Moreover, the short half-life of ^{68}Ga (68 min) makes transport for long distances not feasible, so that expensive ^{68}Ga generators must be therefore installed in the local PET centers. While ^{68}Ga-based tracers are still highly valuable in centers without access to an on-site cyclotron or commercial radiofluoride, sites that do have this option can reduce costs by replacing ^{68}Ga-based tracers with ^{18}F-based tracers.

In addition, the physical properties of ^{68}Ga are not favorable. Sanchez-Crespo (2013). First of all, the short half-life limits the time of scanning to maximum 2 h post-injection, whereas ^{18}F imaging is possible up to 4 h post-injection, allowing for better image contrast. The lower positron yield compared to ^{18}F decreases the sensitivity and the

* Correspondence to: Ghent University Hospital, Nuclear Medicine, Cyclotron Department, De Pintelaan 185, 9000 Gent, Belgium.
E-mail address: ken.kersemans@uzgent.be (K. Kersemans).

https://doi.org/10.1016/j.apradiso.2018.01.006
Received 27 September 2017; Received in revised form 15 December 2017; Accepted 9 January 2018
Available online 12 January 2018
0969-8043/

high partial volume effect renders the quantification of ^{68}Ga PET scans more inaccurate compared to ^{18}F. Finally, the higher energy of the positron reduces the spatial resolution for ^{68}Ga, which is particularly problematic for the detection of small recurrent tumor lesions with limited expression of PSMA (Sanchez-Crespo, 2013).

In contrast to ^{68}Ga, large amounts of [^{18}F]fluoride (typically about 150 GBq) can be provided for radiosynthesis in one cyclotron production and therefore several attempts have been made to introduce a suitable ^{18}F-labeled tracer into hospital routine. Tracers such as ^{18}F-DCFBC (Rowe et al., 2015), ^{18}F-DCFPyl (Wondergema et al., 2017) and more recently ^{18}F-PSMA-1007 (Cardinale et al., 2017) have shown great promise but either feature complex low yielding radiosynthesis, involve precursors with limited availability or are yet to be characterized clinically.

An elegant new approach that recently has gained a lot of attention is the labelling of biomolecules through Al[^{18}F]-chelation. In this method, $^{18}F^-$ is firmly bound to Al^{3+} (> 670 kJ/mol) to form an aluminum fluoride moiety which can be chelated by a suitable chelator (Price and Orvig, 2014). When this chelator is attached to a suitable biomolecule, radiolabelling of a wide variety of complex compounds becomes possible (Price and Orvig, 2014).

McBride and his coworkers were the first to explore this strategy and as a proof of principle they radiolabelled a peptide with Al[^{18}F] using diethylene triaminepentaacetic acid (DTPA) as the chelator (McBride et al., 2009). Despite promising radiochemical yields using a low amount of DTPA-peptide, the formed complexes were not sufficiently stable for in vivo applications (D'Souza et al., 2011). This finding triggered the search for more suitable chelators and both the pentadentate ligand 1,4,7-triazacyclononane-1,4-diacetate (NODA) and the hexadentate ligand 1,4,7-triazacyclononane-1,4,7-triacetic acid (NOTA) were found to form stable complexes with Al[^{18}F]. However, the need for elevated temperatures (100–120 °C) limits their widespread use (McBride et al., 2010).

Meanwhile, the hexadentate ligand N, N-bis(2-hydroxybenzyl) ethylenediamine-N,N-diacetic acid (HBED) gained increased attention as it showed interesting properties towards Al[^{18}F]-based radiolabelling due to its fast chelating kinetics at room temperature and its favorable stability constant (24.8) with aluminum (Yokel and Kostenbauder, 1987). Indeed, Malik et al. (2015) and Boschi et al. (2016) successfully labeled Glu-NH-CO-NH-Lys-(Ahx)-HBED-CC (PSMA-11) with ^{18}F at room temperature in less than 15 min, leading to Glu-NH-CO-NH-Lys-(Ahx)-[Al[^{18}F] (HBED-CC)] (or Al[^{18}F]PSMA-11), hereby succeeding in combining the optimal PET isotope with a proven pharmacophore for PSMA-imaging.

However, despite the existence of successful manual labelling protocols, not a single method has so far been reported to produce large amounts of clinical grade Al[^{18}F]PSMA-11. The aim of this work is to establish an automated radiosynthesis procedure, using a commercially available radiosynthesis platform (Synthra) and readily available reagents that would allow widespread use Al[^{18}F]PSMA-11.

2. Materials and methods

2.1. General

All chemicals were purchased from Sigma-Aldrich (Bornem, Belgium) unless stated otherwise. The precursor, Glu-urea-Lys (Ahx)-HBED-CC (PSMA-11), was purchased from ABX (Radeberg, Germany). $AlCl_3{\cdot}6H_2O$, sodium acetate trihydrate, and acetic acid were all trace metal analysis grade. HPLC eluents, water, acetonitrile, and trifluoroacetic acid (TFA) were of high-grade purity and Ethanol was of Ph. Eur. quality, unless stated otherwise. Ultrapure water was prepared using a Seralpur pro 90 CN system (Belgolabo, Overijse, Belgium). Water for injections (WFI) was obtained from B. Braun Medical N.V. (Diegem, Belgium).

Sep-Pak Accell Plus QMA, Oasis HLB (360 mg) Oasis WCX (360 mg) and Sep-Pak C18-Light cartridges were purchased from Waters (Zellik, Belgium). Alltech Maxi Clean C-18 (300 and 900 mg), Alltech Maxi Clean C18-HC (300 mg) and Alltech Maxi Clean Prevail C18 (900 mg) SPE columns were obtained from Achrom (Machelen, Belgium).

Sodium acetate/acetic acid buffers in concentrations of 0.5 M or 0.05 M with a pH of 4.5 were prepared starting from the 0.5 M or 0.05 M solutions of each component and mixed in suitable ratios to obtain the desired final pH. A phosphate buffer (5 mM, pH 7) was prepared in a similar way starting from sodium phosphate in mono- and dibasic form. PSMA-11 was dissolved in water for injections at a concentration of 1 mg/500 μL and aliquots of 100 μL were stored frozen at −18 °C. A solution of 0.01 M $AlCl_3{\cdot}6H_2O$ was prepared in a 0.05 M acetate buffer of pH 4.5 and stored at 4 °C. Isotonic saline was purchased from GE Healthcare (Diegem, Belgium).

Aqueous (aq.) [^{18}F]fluoride was produced by an ^{18}O (p,n) ^{18}F nuclear reaction with a Cyclone 18/9 cyclotron (IBA, Ghent, Belgium). The enriched [^{18}0]water (97%) for irradiation was obtained from Cambridge Isotope Laboratories (Tewksbury MA, USA). Finally, radioactivity measurements were performed using an Atomlab 100 Plus dose calibrator (Biodex, New York, United States).

2.2. Manual radiosynthesis

2.2.1. General

The papers of Malik et al. (2015) and Boschi et al. (2016) already provide the necessary details for a reliable, yet small scale manual procedure for the radiosynthesis of Al[^{18}F]PSMA-11 and is therefore used as the basis for the optimization of the automated radiochemical procedure. However, several parameters needed further attention prior to upscaling on an automated radiosynthesis platform (Synthra) due to the restrictions that these modules impose with regard to materials, volumes, fractionation etc. The optimal procedure, as described by Boschi was used as a reference and parameters were altered as described below (Boschi et al., 2016).

2.2.2. Optimization of reaction parameters

2.2.2.1. Isolation of [^{18}F]fluoride. For these optimization experiments, freshly produced [^{18}F]fluoride (approximately 2 GBq in 1250 μL of enriched water) was diluted to 12.5 mL with ultrapure water. Samples of 1.250 mL of this dilution were eluted over QMA light columns that were previously preconditioned with 10 mL of an electrolyte (0.5 M solutions of either $NaHCO_3$, $NaNO_3$, NaCl or NaOAc) and subsequently flushed with 10 mL WFI. After trapping of the activity, the QMA light columns were purged to dryness and eluted with each of the aforementioned electrolytes. The eluate was collected in 200 μL fractions and the activity of each fraction and the remaining activity on the QMA column was measured in a dose Calibrator.

2.2.2.2. Formation of the Al-F complex. The formation of the $\{Al^{18}F\}^{2+}$ complex was optimized with regard to the added amount of Al^{3+} and reaction time. For these experiments, a QMA was first conditioned with 10 mL of 0.5 M NaOAc and rinsed with 10 mL of WFI. Freshly produced [^{18}F]fluoride was then trapped on the QMA column. To study the effect of the washing step, the QMA light columns were either flushed with 10 mL of WFI or used without this washing step. The activity was recovered from the column using 0.6 mL of an acetate buffer (0.5 M) of pH 4.5 and 100 μL of this eluate was then diluted in 500 μL of 0.5 M acetate buffer of pH 4.5. Then, an amount of 0, 1, 3, 5, 7, 10 or 25 μL of an $AlCl_3$ solution (0.01 M in 0.05 M acetate buffer of pH 4.5) was added and samples were incubated 10 min at room temperature under gentle shaking. In order to study the time dependency, the experiment was repeated with 10 μL of $ALCl_3$ solution and samples were taken at fixed time points (0.5, 1, 2, 5, 10 and 15 min) to monitor the progress of the complexation reaction. To verify the complexation yields, 5 μL of the reaction mixture was spotted on an a cation exchanger (a preconditioned Oasis WCX column, see earlier). The WCX columns

were then eluted three times with 10 mL of WFI and purged to dryness. The activity on the columns and in the combined water phase was measured in a dose calibrator and the yield was calculated as the percentage of activity on the column relative to the total activity. An amount of 5 μL of freshly eluted [^{18}F]fluoride was used as a negative control to correct for non-specific binding of fluoride to the columns.

2.2.2.3. Optimization of the chelation reaction. Freshly produced [^{18}F]fluoride was trapped on a preconditioned QMA light (Waters) and eluted with 2 mL of electrolyte in a bulk vial. An amount of 25 μg precursor (12.5 μL of the stock solution), 3 μL $AlCl_3$ solution (0.01 M in 0.05 M acetate buffer of pH 4.5), 370–740 MBq Na^{18}F (100 μL taken from the bulk vial), and 150 μL ethanol were mixed and incubated for 10 min at room temperature on a shaking plate. The raw Al[^{18}F]PSMA-11 was trapped on a C18 Sep-Pak light which was then eluted with 0.5 mL ethanol and diluted with 4.5 mL phosphate buffer (2 mM, pH 7). For the optimization of the pH, all parameters were kept the same while the pH of the acetate buffer was varied (either 3.5, 4, 4.5, 5 or 5.5). The experiment was repeated in the absence of ethanol where this solvent was replaced by an equal amount of WFI. In a next experiment, the influence of the relative amount of ethanol to the reaction mixture was studied by varying the volume of added ethanol: either 0, 60, 120, 150 or 200 μL, resulting in ethanol percentages of 0%, 34%, 51%, 57% and 63% (V%). The influence of the molar Al^{3+}/peptide ratio was determined by applying the starting conditions and only varying the amount of added Al^{3+} to the reaction mixture, either 0.7, 13, 2.0, 2.6, 3.3 and 5.2 μL, resulting in molar Al^{3+}/peptide ratios of respectively: 0.25, 0.5, 0.75, 1, 1.25.

A final experiment involved the optimization of the added amount of precursor in an upscaled reaction. An amount of 0.6 mL [^{18}F]fluoride in acetate buffer (0.05 M, pH 4.5) was added to 15 μL of 0.01 M $AlCl_3$ in 0.05 M acetate buffer of pH 4.5 and reacted for 5 min at room temperature. Then 150 μL of PSMA-11 solution (containing either 50, 100, 150 or 200 μg of PSMA-11) and 700 μL EtOH were added and the resulting mixture was allowed to react for 10 min. For all experiments the yields were calculated based on radio-TLC, as described in the quality control section.

2.2.2.4. Purification and formulation. For the purification of the crude reaction mixture, an SPE technique was developed based on the one described by Boschi et al. (2016). To this end following SPE phases were tested: Oasis HLB (360 mg), Sep-Pak C18-Light, Maxi Clean C-18 (300 and 900 mg), Maxi Clean C18-HC (300 mg) and Maxi Clean Prevail C18 (900 mg). All SPE columns were preconditioned using 10 mL of 96% Ethanol, followed by 10 mL of WFI, after which they were purged to dryness.

First, the labelling was performed according to previous paragraph and the radiochemical purity was determined by TLC. To simulate the reaction mixture with minimal activity, 10 μL of the crude reaction mixture was transferred into a recipient and 765 μL of buffer (0.5 M acetate buffer of pH 4.5) was added, followed by 700 μL of 96% ethanol. After homogenisation, the solution was slowly loaded (drop wise) on each of the SPE phases, which were then purged to dryness. Alternatively, 10 μL of the crude reaction mixture was transferred into a recipient to which 765 μL of buffer (0.5 M acetate buffer of pH 4.5), 700 μL of 96% ethanol and 8 mL WFI were added. After homogenisation, the solution was loaded drop wise on each of the SPE phases, which were then purged to dryness. Finally, the second experiment was repeated for the optimal SPE phase with the addition of a washing step consisting of 10 mL of NaCl an 10 mL of WFI to remove traces of unbound fluoride as much as possible.

The activity in the eluate and on the SPE columns was measured using a dose calibrator. The trapped activity was then compared to the expected activity, based on the chemical purity. Additionally, the radiochemical composition of the eluate was determined by TLC.

The recovery of trapped Al[^{18}F]PSMA-11 from the SPE column was assessed by elution with EtOH/WFI 66/34 (V/V) or with 66% EtOH/0.01 M phosphate buffer pH 7(V/V). After recovery, the eluate was diluted to 20 mL to obtain an ethanol concentration of 10%. The solutions for dilution are described below.

2.2.2.5. Shelf life stability testing. The stability of purified Al[^{18}F]PSMA-11 was studied as a function of time in various storage conditions. The reaction was performed using 0.6 mL of [^{18}F]fluoride in acetate buffer (0.05 M, pH 4.5), 15 μL of 0.01 M $AlCl_3$ in 0.05 M acetate buffer of pH 4.5, 150 μL of PSMA-11 solution (containing 150 μg of PSMA-11) and 700 μL EtOH. The mixture was diluted with 8 mL of WFI and sent over an Oasis HLB (360 mg). The Al[^{18}F]PSMA-11 was the eluted with 2 mL of 96% Ethanol from the SPE column and subsequently diluted with 18 mL of either 5 mM Phosphate buffer (pH 7.0), 0.9% NaCl, WFI or 67% EtOH in water. All samples were stored at room temperature or at 5 °C (only the phosphate buffered formulation). At regular time points a 2 μL sample was taken for TLC analysis. Additionally, the loss of the radiolabel after 1 h incubation at room temperature in a 5 mM phosphate buffer of pH 7.0 was studied in function of the concentration of PSMA-11 present.

2.3. Automated radiosynthesis

The automated radiosynthesis of Al[^{18}F]PSMA-11 was performed as a two-step one-pot reaction in a modified SynthraFCHOL synthesis module (Synthra GmbH, Hamburg, Germany) of which the set-up of the module is shown in Fig. 1. Optimized parameters from the manual optimization were programmed into the software and further adjustments to the chemistry, plumbing and programming were made to further optimize the process to allow for GMP-compliant radiosynthesis. In order to be as clear as possible, we describe the optimal configuration and radiosynthesis of Al[^{18}F]PSMA-11 and will then discuss the optimization process.

First of all, the plumbing was made according to Fig. 1, using the standard PTFE tubing (ID of 0.8 mm) that is used in the SynthraFCHOL synthesis module. However, to maximally reduce the flow without the need to insert an additional flow controller, PEEK tubing with an internal diameter of 0.12 mm was used for the connections between reagent vial A2 and valve V3 (30 cm long), between valve 13 and valve 15 (50 cm long) and finally between valve 17 and valve 8 (10 cm long). The target of our cyclotron was connected to our module using PTFE tubing with an ID of 0.8 mm and the outlet of the module is connected to our dispensing unit by means of PTFE tubing with an ID of 1.0 mm.

Prior to irradiation, the cyclotron target and transfer lines, including

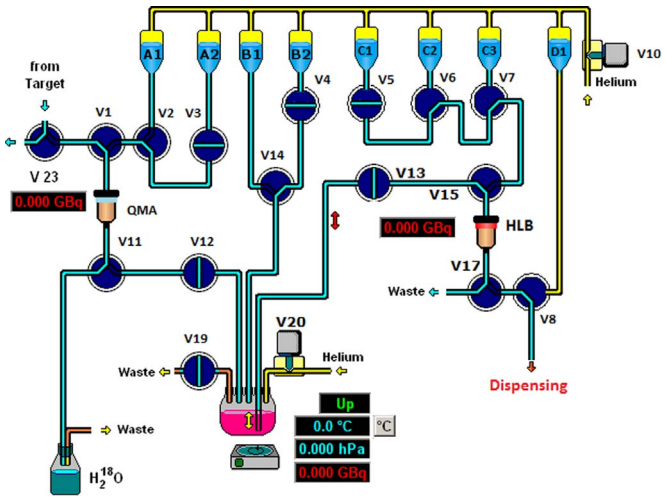

Fig. 1. Schematic representation of the plumbing of the SynthraFCHOL unit for the radiosynthesis of Al[^{18}F]PSMA-11.

the module's internal tubing between V23 and the [^{18}O]H_2O recovery vial are flushed with 500 µL of [^{18}O]H_2O and purged with Helium. This rinsing step minimizes possible accumulation of impurities originating from an earlier productions. After irradiation, the irradiated [^{18}O]H_2O (typically between 80 and 100 GBq) is delivered to the synthesis module and the [^{18}F]fluoride is trapped on an anion exchange cartridge (QMA-light, Waters), which is pre-activated with 0.5 M NaOAc (10 mL) and water (10 mL). The QMA is then washed with 25 mL WFI from A1 to the recovery vial. The [^{18}F]fluoride is then eluted with 0.6 mL acetate buffer (0.05 M, pH 4.5) into the reactor which is preloaded with 10 µL of 0.01 M $AlCl_3$ in 0.05 M acetate buffer of pH 4.5. The reactor is closed and the mixture is allowed to react for 5 min at room temperature, after which the precursor solution, a mixture of 150 µL PSMA-11 (containing 200 µg of precursor) and 700 µL EtOH, is added to the reactor via valve 14. All valves are closed again and the reaction mixture is allowed to react for 10 min at room temperature. When the labelling is complete, the reaction mixture is diluted with 8 mL WFI and passed over two Oasis HLB mini-columns in tandem, hereby trapping the Al[^{18}F]PSMA-11. Subsequently, the trapped product is then washed with 10 mL 0.9% NaCl and 10 mL WFI and then purged to dryness. The product is then eluted from the mini-column into the bulk vial (preloaded with 20 mL of 5 mM phosphate buffer of pH 7.0) in the dispensing hotcell with 3 mL of EtOH/phosphate buffer (5 mM, pH 7.0) 67/33 (v/v). After completion of the transfer, the lines are purged with 4 mL of phosphate buffer (5 mM, pH 7.0). After homogenisation by manual shaking, the formulation is ready for dispensing and use.

An important side note with regard to the set-up of the synthesis module is related to the recovery of the enriched water. In order to reduce costs, an extra valve may be installed between V11 and the recovery vial. This will allow to isolate the enriched water which can be submitted for reprocessing.

2.4. Quality control

Radiochemical purity and activity/peptide ratio (total activity in MBq divided by the total amount of peptide in mmoles) of Al[^{18}F]PSMA-11 were determined by analytical high-performance liquid chromatography (HPLC) using an Agilent 1260 infinity system (Agilent Technologies, Diegem, Belgium) consisting of a quaternary pump, an auto-sampler and a column oven. Ultraviolet (UV) absorption was detected with an Agilent 1260 variable wavelength detector at a wavelength of 220 nm in series with a Raytest “Gabi Star” detector (Elysia-Raytest, Liège, Belgium) for radioactivity detection. As stationary phase a Prevail C18 (4.6 × 250 mm, 5 µ, Lokeren, Belgium) was used at 40 °C. As mobile phase a gradient system (Solvent A: water (0.1%) TFA; Solvent B: acetonitrile (0.1% TFA); between 0 and 4 min: 15% B, between 4 and 11 min: from 15% B to 70%, between 11 and 14 min from 70% B to 15% B and between 14 and 16 min: 15% B) was used with a flow rate of 2 mL/min. The radiochemical purity was also determined by TLC using Alugram RP18-W/UV254 plates (Machery Nagel, Düren, Germany) and 70% acetonitrile in water as mobile phase and a Raytest MiniGitaTLC scanner for detection of the radioactive spots. Endotoxins were determined using the Endosafe PTS system (Charles-River, Charleston, USA). Residual aluminum was determined using the Tec-Control Breakthru Kit (Biodex, Groningen, The Netherlands). The pH of al final formulations was checked using Paper dosatest pH 4.5–10.0 strips (VWR-international, Oud-Heverlee, Belgium).

3. Results and discussion

3.1. Manual radiosynthesis of Al[^{18}F]PSMA-11

For the manual radiosynthesis we used the work of Malik and Boshi as a reference and then optimized and upscaled individual parameters to fit the needs of our automated system (Malik et al., 2015; Boschi et al., 2016). Each essential reaction step and parameter is sequentially discussed below.

3.1.1. Isolation of [^{18}F]fluoride

In previous work, the radiofluorine that is coming from the QMA during elution is fractionated (typically 100 µL/fraction) after which the most active fraction is identified and then used for radiolabelling (Malik et al., 2015; Boschi et al., 2016). This accomplishes two things: firstly, the radiofluorine is recovered in the highest possible activity per volume and the bulk of impurities (metal ions) that elute with the solvent front are avoided. This elegant method plays a crucial role in achieving the high yields that are associated with the manual procedure but is hard to implement in an automated module. In an effort to translate this strategy to an automated procedure, several different approaches were tried including the use of dilute electrolyte solutions and gradient elutions. However, these strategies were found to be too impractical (i.e. large elution volumes) or lead to highly variable results, hampering the reproducibility of the method. Therefore, to keep the method as simple as possible, we aimed to develop a straightforward elution method, using an appropriate volume of the most suitable electrolyte for subsequent radiolabelling, without the need of fractionation.

First the retention of radiofluorine was studied on QMA light columns that were preconditioned with different electrolytes ($NaHCO_3$, $NaNO_3$, NaCl or NaOAc). In all cases, radiofluorine was trapped with an efficiency exceeding 99.9%. However, different elution patterns were observed when the same electrolytes were used to displace the radiofluorine from the anion exchanger (shown in Fig. 2). From this graph it becomes clear that, with regard to a fractionated approach, 0.9% NaCl obviously is the electrolyte of choice as the first 200 µL can be discarded and the bulk of the activity can be recovered in the second fraction of 200 µL. However, the recovery of radiofluorine from the QMA column is nearly quantitative for all electrolytes when a total unfractionated elution volume of 600 µL is used. When these solutions were then used for subsequent radiolabelling (shown in Table 1), the acetate buffer of pH 4.5 showed the best radiochemical yield and was therefore retained for further optimization.

Next, the wash step following the trapping of the radiofluorine was optimized. Low, irreproducible yields were observed when the column was not flushed with WFI. Slightly better, but highly variable yields were obtained when the QMA was flushed with 10 mL of WFI. However, when we used 25 mL of WFI, labelling yields remained constant and these did not improve by increasing the amount of WFI for washing.

Based on aforementioned observations, we propose a QMA light that is preconditioned with 10 mL of 0.5 M acetate buffer and rinsed with 10 mL WFI prior to use. After trapping of the freshly irradiated fluorine (about 100 GBq in 2000 µL), the QMA should be rinsed with 25 mL of WFI and purged to dryness using a Helium flow. The

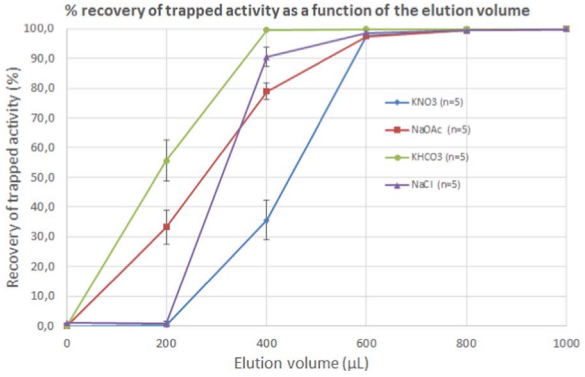

Fig. 2. Elution patterns of [^{18}F]fluoride from a QMA-light, using 0.5 M solutions of either $NaHCO_3$, $NaNO_3$, NaCl or NaOAc in WFI. The recovery of the trapped radioactivity, expressed as the % of the total activity (n = 5) is plotted as a function of the elution volume.

Table 1
Summary of the QC tests and results for the validation runs (n = 3) of the automated radiosynthesis of Al[^{18}F]PSMA-11. (Starting activity ± 100 GBq).

Measured parameter	Method/Equipement	Validation approach	Results (N = 3)
Activity	Dose calibrator	Methodology for validation and control testing of dose calibrators is based on the IAEA guidelines for nuclear medicine instruments.	24.0 ± 6.0 GBq
Appearance	Visual inspection	Visual inspection of the content of the vial as described in Ph. Int. methods of analysis chapter as applied to radiopharmaceuticals.	Conform
Acidity/Alkalinity	pH paper	Direct pH measurement based on colour indicator.	7.0 ± 0.1
Identity	HPLC with UV and radioactivity detection	Identification of the radioactive compound by HPLC using co-elution technique. Retention times between radioactive product and reference standard are compared. Detection by UV-spectrometry at 220 nm and radioactivity detection.	Conform
Radiochemical purity by TLC	TLC - radiodetection	Reversed Phase TLC eluted with AcN/Water 70/30 solution. Separation of fluoride and Al[^{18}F]PSMA − 11 was demonstrated with high resolution and reproducibility.	97 ± 2%
Radiochemical and chemical purity by HPLC	HPLC with UV and radiodetection	Method based on methodology developed by Malik et al. Validation according to ICH guidelines for analytical procedures as applied to testing for impurities. Validation includes specificity, detection limit, robustness and repeatability of the method.	Radiochemical Purity: 97.5 ± 0.3% Chemical Purity: < 20 μg/V
Chemical purity: Aluminum	Colorimetry	Method based on the Aluminum breakthrough kit (Biodex)	< 20 μg/V
Radionuclidic identity and purity: half-life	Dose calibrator	Methodology as described in Ph. Eur. as applied to short-lived radiopharmaceuticals.	111.3 ± 2.8
Radionuclidic identity and purity: Eγ	Gamma-spectrometry	Methodology as described in Ph. Eur. as applied to short-lived radiopharmaceuticals.	512.9 ± 4.0 keV
Radio-nuclidic purity (long lived impurities)	Gamma-spectrometry	Methodology as described in Ph. Eur. as applied to short-lived radiopharmaceuticals.	< 0.1%
Bacterial endotoxins	LAL-test	Method with reference to Ph. Eur. 2.6.14.	< 10 EU/V
Sterility	Membrane filtration	Method with reference to Ph. Eur. 2.6.1.	Sterile

radiofluorine can then be eluted almost quantitatively with 600 μL of 0.5 M acetate buffer pH 4.5.

3.1.2. Formation of the Al-F complex

The key step in the radiolabelling of PSMA-11 is the formation of the complex between aluminum and fluoride leading to the aluminum fluoride moiety where $^{18}F^-$ is firmly bound to Al^{3+} (> 670 kJ/mol). Literature suggests that when fluoride is present in low concentrations relative to Al^{3+}, mainly monofluoride species ($\{AlF\}^{2+}$) are formed and as the concentration of fluoride increases, a series of AlF_n^{3-n} species can be observed, where n ranges from one to six (Price and Orvig, 2014). However, it is only the $\{AlF\}^{2+}$ species that can be efficiently chelated by the HBED chelator (Price and Orvig, 2014). Therefore we optimized the required amount of Al^{3+} and defined the minimal time that is required to form the Al-F complex. These data are summarized in Fig. 3. From these data it becomes clear that up from 70 nanomoles of Al^{3+} no additional benefit is observed with regard to the amount of $\{Al^{18}F\}^{2+}$ that can be formed. When the formation of $\{Al^{18}F\}^{2+}$ is compared between "clean" QMA columns (washed with 25 mL WFI after trapping of the radiofluoride) or "dirty" ones (eluted right after trapping), the influence of the wash step becomes clear: $\{Al^{18}F\}^{2+}$ formation is 9% higher when a wash step is included. When the yield of the complex formation is plotted as a function of time, it becomes clear that a plateau is reached after 2 min. In order to reduce the effects due to timing and pipetting errors, an amount of 100 nmol and an incubation time of 5 min was used for future experiments.

3.1.3. Optimization of the chelation reaction

Aluminum forms octahedral complexes, requiring hexadentate ligands for optimal binding (Malati, 1999). However, as we use the HBED chelator of PSMA-11, which is also used for the complexation of Gallium-68, one dentate will be free as the fluoride occupies the sixth position of the complex (McBride et al., 2009; D'Souza et al., 2011). For radiolabelling this poses no problem, as was proven in earlier work (Malik et al., 2015; Boschi et al., 2016). This will, however, have an effect on the stability of the final complex which will be discussed below. As was proven before, the chelation process depends on pH, (relative amounts) of reagents, temperature and the type and amount of co-solvent that is used in the complexation reaction. Moreover, as has been alluded before, metallic impurities coming from the target should also be considered. Last but not least, the order in which reagents are added to the reactor is also taken into account as an automated procedure is limited by restrictions inherent to an automated module.

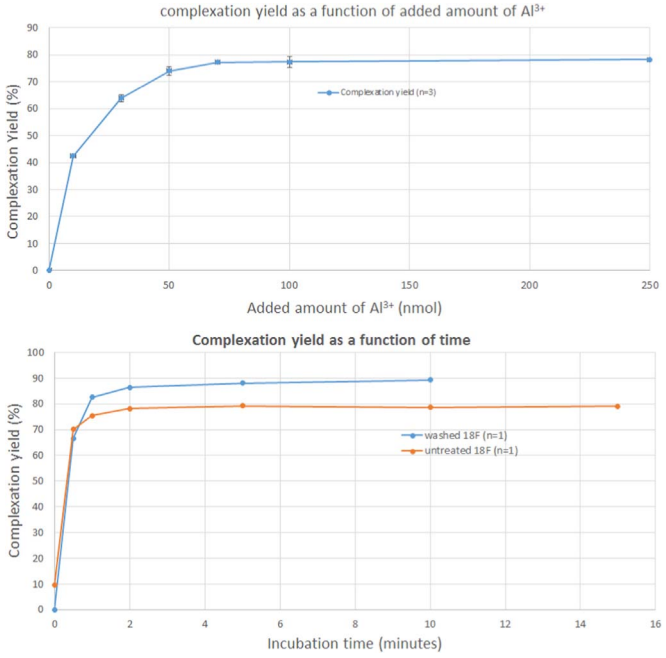

Fig. 3. Complexation yields (n = 3) after 5 min of incubation at room temperature as a function of the added amount of Al^{3+} for untreated [^{18}F]fluoride (upper graph). Complexation yields (n = 1) as a function of time for washed and untreated [^{18}F]fluoride (lower graph) using 20 μL of.

As is clear from Fig. 4, the optimal pH for the chelation process is 4.5, which is consistent with previous reports. In this context it is important to point out that the choice of electrolyte for the elution of the QMA column plays an important role as it might substantially change the pH of the final mixture, especially since it represents roughly 50% of the total volume. Moreover, when too dilute acetate buffers are used, a slight shift in pH can be observed due to the addition of the reagents. Therefore we opted to elute the activity with 600 μL of an acetate buffer of pH 4.5 with a buffer concentration of 0.05 M.

Secondly we studied the effect of the amount of co-solvent on the

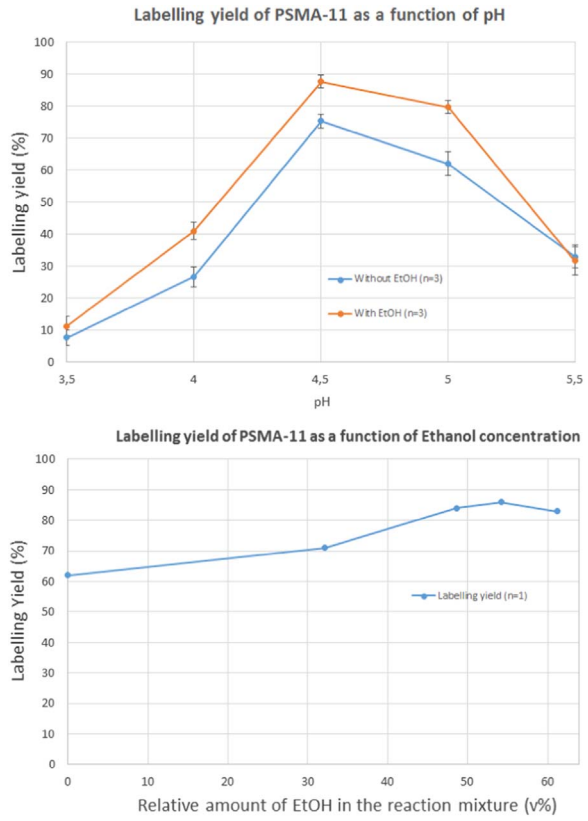

Fig. 4. Labelling yields (n = 1) of Al[^{18}F]PSMA-11 as a function of pH. Reactions were performed as described under Section 2.2 and only the pH of the Acetate buffer was varied. In a second experiment (blue line) EtOH was replaced by 150 µL water and the pH of the Acetate buffer was varied (Upper Graph). The lower graph shows the labelling yield as a function of the relative amount of ethanol in the reaction mixture (in V%) for reactions were performed as described under Section 2.2 with the added volume of EtOH as the only variable.

reaction mixture. We only studied the yield as a function of the amount of ethanol due to its compatibility with human applications. A marked increase in labelling yield can be observed with increasing ethanol concentrations but at about 50% a plateau is reached. In order to facilitate the preconcentration step we aimed to keep the amount of ethanol to a minimum and opted to add 600 µL to the reaction mixture, resulting in a 48.6% ethanol in water (v%) concentration.

From Fig. 5 it becomes apparent that the labelling yield increases

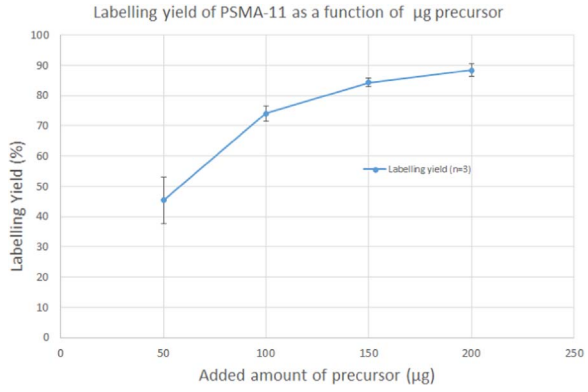

Fig. 5. Manual labelling yields (relative to the total amount of activity added, n = 3) as a function of added amount of precursor. Reaction parameters: 0.6 mL [^{18}F]fluoride in acetate buffer (0.05 M, pH 4.5) was added to 15 µL of 0.01 M $AlCl_3$ in 0.05 M acetate buffer of pH 4.5 and reacted for 5 min at room temperature. Then 150 µL of PSMA-11 solution (mass was varied) was added together with 700 µL of EtOH and the mixture was incubated for 10 min at room temperature.

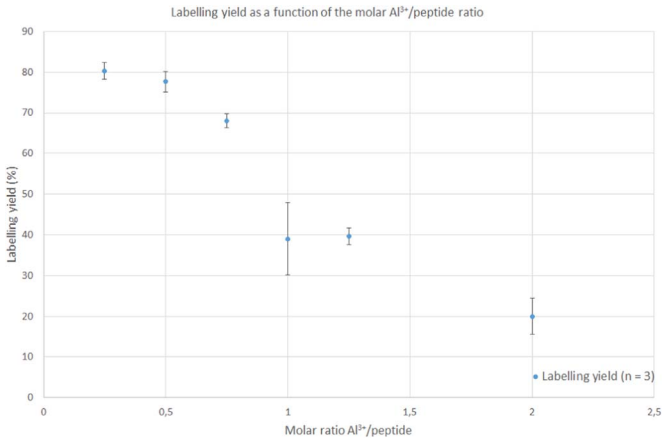

Fig. 6. Labelling yields (n = 3) as a function of the molar Al^{3+}/peptide ratio. Reactions were performed as described under Section 2.2, using a fixed amount of precursor while varying the amount of added Al^{3+}.

with the amount of precursor added, as can be expected. However, while it is tempting to use more precursor to force the reaction to even higher yields and to minimize the effect of competing metallic impurities coming from the cyclotron, it should be noted that this comes at a drastic increase in cost due to the expensive precursor. Moreover, as micro-dosing is preferred for radiotracers with regard to safety and regulatory issues, it is advisable to keep concentrations to a strict minimum. We opted to apply a maximum of 200 µg PSMA-11 for each synthesis as in our experience this provides a sufficient good yield and an excellent reproducibility. When we lowered the amount of precursor to 150 µg we sometimes experienced reduced yields (up to 30% less), which are most likely due to fluctuating amounts of metallic impurities originating from the target material.

The last parameter to be considered is the relative amount of Al^{3+} that is added to the reaction mixture. The optimization of this parameter is shown in Fig. 6. When the molar Al^{3+}/peptide ratio drops below 0.5, an apparent plateau is reached, which is in line with the findings of Cleeren et. al. on the very similar RESCA1 chelator (Pillarsetty et al., 2016; Charlot, 1983). Based on these observations and the results from preceding formation of the Al-F complex, we propose a ratio of 0.5 (amounting to 100 nanomoles of Al^{3+} for a reaction with 200 µg of PSMA-11) for maximum yields and reproducibility.

An important side note is related to the quality and shelf-life of the used precursor. We noticed that after 6 months, the labelling yield was cut to half as compared to a fresh batch of precursor. Concomitantly, during QC HPLC analysis, a reduced chemical purity can be observed when old precursor was used for the radiosynthesis (data not shown). Keeping a large stock of precursor in the freezer is hence not recommended. Finally, it is also recommended to use GMP-grade PSMA-11 (from ABX, Radeberg, Germany) for the automated radiosynthesis as it results in a higher radiochemical purity of the final preparation. This is due to the presence of an unidentified additional peak on the HPLC radiochromatogram when non-GMP grade PSMA-11 was used for radiolabelling, as is clear from the selected chromatograms shown in Fig. 7.

3.1.4. *Purification and formulation*

The next important step is the purification of the reaction mixture. We opted to adapt the earlier described preconcentration technique (Boschi et al., 2016) as it is a simple and fast method. However, some changes were required as straightforward application of the protocol lead to loss of product-activity up to 50% for all tested SPE columns. These losses are related to the increase in reaction volume leading to a mismatch with the stationary phase. We opted to dilute the mixture with 8 mL WFI prior to concentration, leading to a final ethanol

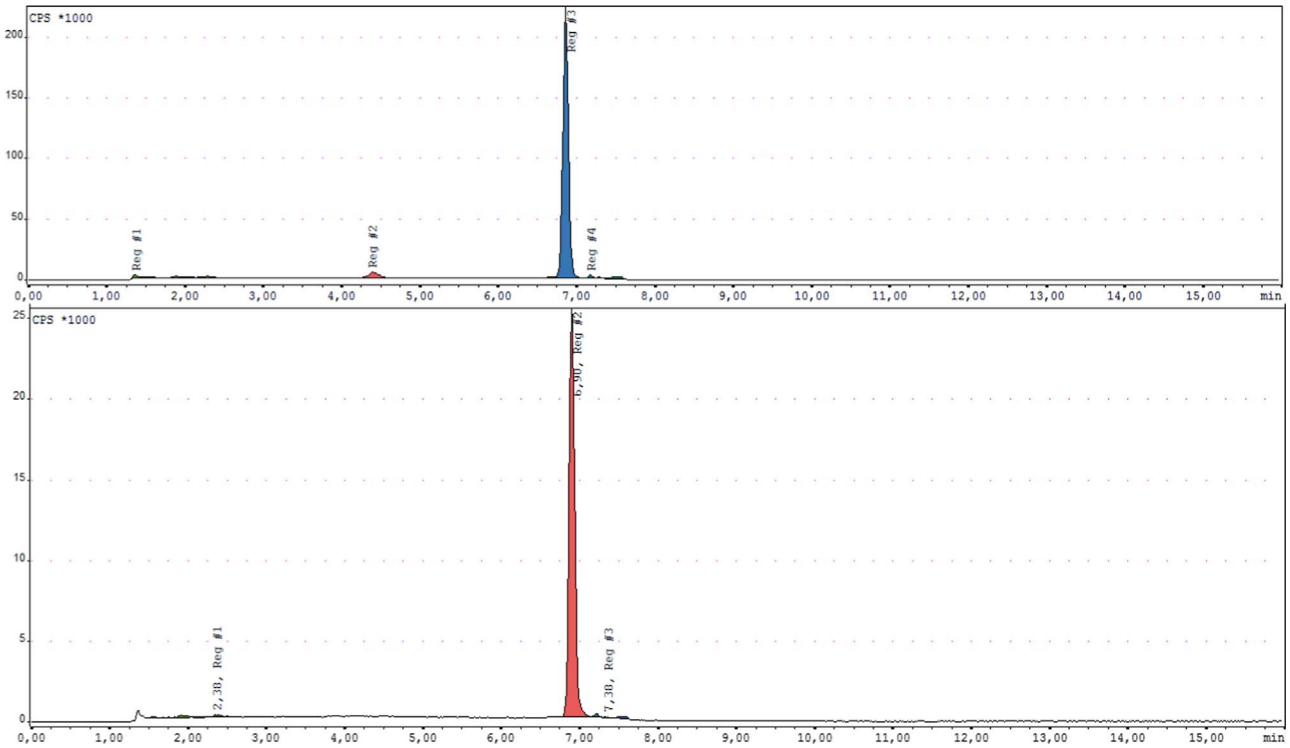

Fig. 7. Radiochromatograms obtained from the quality control by HPLC of freshly produced Al[^{18}F]PSMA-11 using either the regular PSMA-11 (upper graph) or GMP-quality PSMA-11 precursor from ABX (Radeberg, Germany).

concentration of 7.5% (V%), in order to increase the retention of Al[^{18}F]PSMA-11 on the stationary phase. Seven different SPE systems were evaluated for their retention behavior in these conditions. The Sep-Pak C18 Plus Light, Alltech Maxi Clean C18 (300 mg and 900 mg), Alltech Maxi Clean HC C18 (300 mg) systems were immediately discarded as more than 30% of product-activity was lost during the preconcentration step. The Waters Sep-Pak C18 Plus Short column was also discarded as breakthrough of Al[^{18}F]PSMA-11 was observed during the washing step. Only the Oasis HLB and the Alltech Maxi Clean Prevail C18 (300 mg) showed good retention (> 75% for a single column and > 98% with two columns in tandem) with no significant breakthrough of Al[^{18}F]PSMA-11 during the washing step. Finally the activity could successfully be recovered (recovery > 98%) from both SPE column systems by elution with 3 mL of EtOH/WFI 66/34 (V/V). Following the stability study this was changed to 3 mL of 66% EtOH/0.01 M phosphate buffer pH 7(V/V) for reasons discussed below. Despite the good trapping efficiency, the Prevail C18 phase was not preferred due to the observed higher back-pressure and resulting slow flow rate in our automatic system, as compared to the HLB columns. Hence we propose two HLB (360 mg) SPE columns in tandem for the purification of Al[^{18}F]PSMA-11.

3.1.5. Shelf life stability testing

As stated earlier, the free (sixth) dentate of the HBED chelator is a point of concern as it could compete with [^{18}F]fluoride for binding on the aluminum ion. Limited data is available on the stability of Al[^{18}F]PSMA-11 (Malik et al., 2015; Boschi et al., 2016). So far it was accepted that a radiochemical purity of > 97% was observed in buffered solution at pH 6.8 in comparison with unbuffered saline formulation, which showed a roughly 20% decrease in radiochemical purity after 3 h (Boschi et al., 2016). Our in depth study of the stability is shown in Fig. 8. These data suggest that the stability is clearly dependent on the temperature (entropy effect), the type of buffer (which also competes with the chelator) and the dilution factor of the original formulation. Buffer systems that include components that feature an important

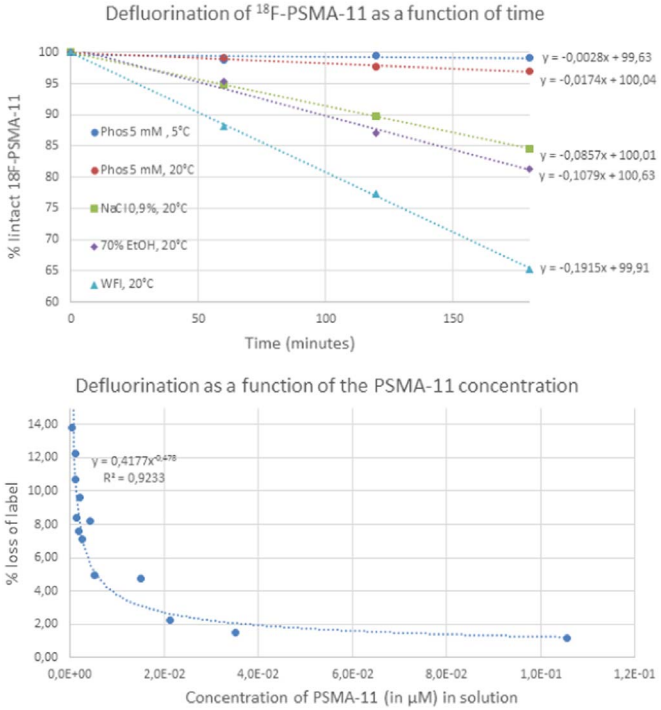

Fig. 8. Stability of Al[^{18}F]PSMA-11 as a function of time in various storage conditions. (Upper graph). Loss of the radiolabel after 1 h incubation at room temperature in a 5 mM phosphate buffer of pH 7.0 plotted in function of the concentration of PSMA-11 present (Lower graph).

complexation constants, e.g. citrate (Pk_1 = 7.0), with Aluminum should be avoided (Charlot, 1983). Despite the weak complexation constant of $H_2PO_4^-$ with Aluminum (pK_1 = 2.1) we propose a phosphate buffer of 5 mM at pH 7, with a final formulation volume of maximally 30 mL. When stored under these conditions at room temperature, the

compound was stable (less than 5% loss of label) for at least 4 h. When the compound is to be distributed to peripheral institutions, we suggest to keep the stock solution refrigerated as no significant loss of the radiolabel was observed in these conditions for at least 6 h.

3.2. Automated radiosynthesis

The most important factor in the automatization of the radiosynthesis is the sequence in which the reagents are added. It may be tempting to simplify the procedure, hereby reducing the complexity (and cost) of the synthesis module. The simplest set-up would be to load the reactor with the precursor- and Al^{3+} solution, followed by elution of the radiofluoride into the reactor. However, it was found that this approach leads to low radiochemical yields and the formation of an unstable radiolabeled compound which is most likely a diastereoisomer of the desired compound. A similar phenomenon has already been observed by McBride et al. (2010) for the chelation of AlF^{2+} by the NOTA chelator. The appearance of this diastereoisomer is probably due to the formation of a HBED-Al^{3+}complex with a different geometry prior to the addition of the radiofluorine, leading to a different final complex than when preformed AlF^{2+} is allowed to react with the HBED chelator.

Nevertheless, when the radiofluorine is incubated with Al^{3+} for 5 min prior to addition of the precursor, followed by an additional incubation to bind the Al-F complex to the HBED chelator of the precursor, the undesired compound is no longer observed and reproducible high yields of Al[^{18}F]PSMA-11 are obtained. Moreover, all manually optimized parameters can be applied without further modifications. The described automated method yields 21 ± 3% (not corrected for decay) of Al[^{18}F]PSMA-11 within 35 min. This yield is much lower than observed for the described manual radiosynthesis procedures, which is probably due to the fact that the automated system does not discard a fraction of the eluate coming from the QMA. While the rinsing step with 25 mL is thought to remove impurities coming from the target, it is highly probable that traces persist. Moreover, as the total elution volume ends up in the reactor, relatively higher levels of metal ions are suspected to be present in the reactor that can impede the chelation of AlF^{2+}. Moreover, as metallic sharps are used in the automated system, as opposed to the manual syntheses, it is not excluded that they also influence the radiolabelling yield negatively. Despite this consideration, using the described automated radiosynthesis, we were able to produce batches up to 30 GBq of Al[^{18}F]PSMA-11, which will allow large scale application of this tracer.

Quality control parameters of batches produced thus far (meanwhile more than 50) show that high-quality Al[^{18}F]PSMA-11 can be produced using the described method. Moreover, the activity/peptide ratio of Al[^{18}F]PSMA-11 (120 ± 28 GBq/μmol) is similar to the earlier described NOTA analogue (McBride et al., 2010) and superior to that of ^{68}Ga-PSMA-11 (Pillarsetty et al., 2016). Meanwhile our cyclotron site at the campus of the University Hospital Ghent (Belgium) has acquired GMP-accreditation for the production of Al[^{18}F]PSMA-11 and the compound is meanwhile being studied in a large scale prospective clinical trial. The QC data of the validation runs are shown below in Table 1.

Our final comments are related to the future radiolabeled compounds aimed at PSMA. Interestingly, Cleeren et. al. (2016, 2017) recently developed the more stable RESCA1 chelator for the radiolabelling of biomolecules with AlF^{2+}. This chelator holds great promise for further improvement of this radiolabelling strategy and PSMA-RESCA1 could replace PSMA-11 as the precursor of choice for the production of a radiofluorinated PSMA based compound once it has been sufficiently characterized preclinically and when it becomes freely available. Due to the similarity between PSMA-RESCA1 and PSMA-11, we expect that the optimized parameters and set-up of the automated module that are described in this paper can also be applied for this new chelator, ensuring a long term applicability of this methodology.

4. Conclusion

The optimized synthesis of Al[^{18}F]PSMA-11 using a SynthraFCHOL module allows for large scale production of Al[^{18}F]PSMA-11 (21% ± 3% e.o.s.), suitable for clinical routine. Moreover, this method can be applied in a GMP setting and is expected to be compatible with the new chelators that are currently being developed. We expect that widespread use of this technology will have a beneficial impact on prostate cancer diagnosis worldwide as large populations of patients can be processed faster and at a reduced cost, relative to ^{68}Ga-based radiotracers.

References

Aus, G., Abbou, C.C., Bolla, M., Heidenreich, A.P., Van Poppel, H., Wolff, J., Zattoni, F., 2005. EAU guidelines on prostate cancer. Eur. Urol. 48, 546–551.

Bander, N.H., 2006. Technology insight: monoclonal antibody imaging of prostate cancer. Nat. Clin. Pract. Urol. 3, 216–225.

Boschi, S., Lee, J.T., Beykan, S., Slavik, R., Wei, L., Spick, C., Eberlein, U., Buck, A.K., Lodi, F., Cicoria, G., Czernin, J., Lassmann, M., Fanti, S., Herrmann, K., 2016. Eur. J. Nucl. Med. Mol. Imaging 43, 2122–2130.

Cardinale, J., Schäfer, M., Benešová, M., Bauder-Wüst, U., Leotta, K., Eder, M., Neels, O.C., Haberkorn, U., Giesel, F.L., Kopka, K., 2017. J. Nucl. Med. 58 (3), 425–431.

Charlot, G., 1983. Les Réactions chimiques en solution aqueuse et caractérisation des ions, 7th ed. Masson, pp. 190.

Cleeren, F., Lecina, J., Billaud, E.M.F., Ahamed, M., Verbruggen, A., Bormans, G.M., 2016. New chelators for low temperature Al^{18}F-labeling of biomolecules. Bioconjug. Chem. 27 (3), 790–798.

Cleeren, F., Lecina, J., Ahamed, M., Raes, G., Devoogdt, N., Caveliers, V., McQuade, P., Rubins, D.J., Li, W., Verbruggen, A., Xavier, C., Bormans, G., 2017. Al^{18}F-labeling of heat-sensitive biomolecules for positron emission tomography imaging. Theranostics 7 (11), 2924–2939.

D'Souza, C.A., McBride, W.J., Sharkey, R.M., Todaro, L.J., Goldenberg, D.M., 2011. High-yielding aqueous ^{18}F-labeling of peptides via Al^{18}F chelation. Bioconjug. Chem. 22, 1793–1803.

Eder, M., Schäfer, M., Bauder-Wüst, U., Hull, W.E., Wängler, C., Mier, W., Haberkorn, U., Eisenhut, M., 2012. ^{68}Ga-complex lipophilicity and the targeting property of a urea-based PSMA inhibitor for PET imaging. Bioconjug. Chem. 23, 688–697.

Hillier, S.M., Maresca, K.P., Femia, F.J., Marquis, J.C., Foss, C.A., Nguyen, N., Zimmerman, C.N., Barrett, J.A., Eckelman, W.C., Pomper, M.G., Joyal, J.L., Babich, J.W., 2009. Preclinical evaluation of novel glutamate-urea-lysine analogues that target prostate-specific membrane antigen as molecular imaging pharmaceuticals for prostate cancer. Cancer Res. 69, 6932–6940.

Liu, H., Moy, P., Kim, S., Xia, Y., Rajasekaran, A., Navarro, V., Knudsen, B., Bander, N.H., 1997. Monoclonal antibodies to the extracellular domain of prostate-specific membrane antigen also react with tumor vascular endotHelium. Cancer Res. 57, 3629–3634.

Malati, M.A., 1999. Experimental Inorganic/Physical Chemistry, 1st ed. pp. 66.

Malik, N., Baur, B., Winter, G., Reske, S.N., Beer, A.J., Solbach, C., 2015. Radiofluorination of PSMA-HBED via Al^{18}F^{2+} chelation and biological evaluations in vitro. Mol. Imaging Biol. 17, 777–785.

Mannweiler, S., Amersdorfer, P., Trajanoski, S., Terrett, J.A., King, D., Mehes, G., 2009. Heterogeneity of prostate-specific membrane antigen (PSMA) expression in prostate carcinoma with distant metastasis. Pathol. Oncol. Res. 15, 167–172.

Maurer, T., Eiber, M., Schwaiger, M., Gschwend, J.E., 2016. Current use of PSMA-PET in prostate cancer management. Nat. Rev. Urol. 13 (4), 226–235.

McBride, W.J., Sharkey, R.M., Karacay, H., D'Souza, C.A., Rossi, E.A., Laverman, P., Chang, C.-H., Boerman, O.C., Goldenberg, D.M., 2009. A novel method of ^{18}F radiolabeling for PET. J. Nucl. Med. 50, 991–998.

McBride, W.J., D'Souza, C.A., Sharkey, R.M., Karacay, H., Rossi, E.A., Chang, C., Goldenberg, D.M., 2010. Improved 18F labeling of peptides with a fluoride-aluminum-chelate complex. Bioconjug. Chem. 21 (7), 1331–1340.

Pillarsetty, N., Kalidindi, T., Carlin, S., Easwaramoorthy, B., Abbasi, A., Larson, S., Osborne, J., Weber, W., 2016. Effect of specific activity on the uptake of [^{68}Ga]DKFZ-PSMA-11 in tumor and other organs. J. Nucl. Med. 57 (Suppl 2), S528.

Price, E.W., Orvig, C., 2014. Matching chelators to radiometals for radiopharmaceuticals. Chem. Soc. Rev. 43, 260–290.

Rowe, S.P., Gage, K.L., Faraj, S.F., Macura, K.J., Cornish, T.C., Gonzalez-Roibon, N., Guner, G., Munari, E., Partin, A.W., Pavlovich, C.P., Han, M., Carter, H.B., Bivalacqua, T.J., Blackford, A., Holt, D., Dannals, R.F., Netto, G.J., Lodge, M.A., Mease, R.C., Pomper, M.G., Cho, S.Y., 2015. ^{18}F-DCFBC PET/CT for PSMA-based detection and characterization of primary prostate cancer. J. Nucl. Med. 56 (7), 1003–1010.

Sanchez-Crespo, A., 2013. Comparison of gallium-68 and fluorine-18 imaging characteristics in positron emission tomography. Appl. Radiat. Isot. 76, 55–62.

Schäfer, M., Bauder-Wüst, U., Leotta, K., Zoller, F., Mier, W., Haberkorn, U., Eisenhut, M., Eder, M., 2012. A dimerized urea-based inhibitor of the prostate-specific membrane antigen for ^{68}Ga-PET imaging of prostate cancer. EJNMMI Res. 2, 23.

Stewart, B.W., Wild, C.P., 2014. World Cancer Report 2014. International Agency for Research on Cancer (ISBN-13 978-92-832-0429-9).

Sweat, S.D., Pacelli, A., Murphy, G.P., Bostwick, D.G., 1998. Prostate-specific membrane

antigen expression is greatest in prostate adenocarcinoma and lymph node metastases. Urology 52, 637–640.
Wondergema, M., van der Zanta, F.M., Knola, R.J.J., Lazarenko, S.V., Pruim, J., de Jong, I.J., 2017. ^{18}F-DCFPyL PET/CT in the detection of prostate cancer at 60 and 120 min; detection rate, image quality, activity kinetics and biodistribution. Nucl. Med (April 27, 2017.jnumed.117.192658).
Yokel, R.A., Kostenbauder, H.B., 1987. Assessment of potential aluminum chelators in an octanol/aqueous system and in the aluminum-loaded rabbit. Toxicol. Appl. Pharmacol. 91 (2), 281–294.